Neurobiology of Aging 96 (2020) 137–147

Contents lists available at ScienceDirect

Neurobiology of Aging

journal homepage: www.elsevier.com/locate/neuaging

Multimodal in vivo and postmortem assessments of tau in Lewy body disorders

David G. Coughlin[a,b,c], Jeffrey S. Phillips[a,d], Emily Roll[a,d], Claire Peterson[b], Rebecca Lobrovich[b], Katya Rascovsky[a,d], Molly Ungrady[a,d], David A. Wolk[a,e], Sandhitsu Das[a,e], Daniel Weintraub[a,f], Edward B. Lee[e,g], John Q. Trojanowski[a,e,g,h], Leslie M. Shaw[g], Sanjeev Vaishnavi[a,c], Andrew Siderowf[a,c], Ilya M. Nasrallah[i], David J. Irwin[a,b,c,d], Corey T. McMillan[a,d,*], for the Alzheimer's Disease Neuroimaging Initiative[1]

[a] Department of Neurology, Hospital of the University of Pennsylvania, Philadelphia, PA, USA
[b] Digital Neuropathology Laboratory, Perelman School of Medicine at the University of Pennsylvania, Philadelphia, PA, USA
[c] Lewy Body Disease Center of Excellence, Perelman School of Medicine at the University of Pennsylvania, Philadelphia, PA, USA
[d] Frontotemporal Degeneration Center, Perelman School of Medicine at the University of Pennsylvania, Philadelphia, PA, USA
[e] Alzheimer's Disease Center, Perelman School of Medicine at the University of Pennsylvania, Philadelphia, PA, USA
[f] Michael J. Crescenz VA Medical Center, Parkinson's Disease Research, Education, and Clinical Center, Philadelphia, PA, USA
[g] Department of Pathology, Hospital of the University of Pennsylvania, Philadelphia, PA, USA
[h] Center for Neurodegenerative Disease Research, Hospital of the University of Pennsylvania, Philadelphia, PA, USA
[i] Department of Radiology, Hospital of the University of Pennsylvania, Philadelphia, PA, USA

ARTICLE INFO

Article history:
Received 13 January 2020
Received in revised form 30 July 2020
Accepted 3 August 2020
Available online 21 August 2020

Keywords:
Lewy body diseases
PET imaging
Tau
CSF
Cognition
Neuropathology

ABSTRACT

We compared regional retention of ^{18}F-flortaucipir between 20 patients with Lewy body disorders (LBD), 12 Alzheimer's disease patients with positive amyloid positron emission tomography (PET) scans (AD+Aβ) and 15 healthy controls with negative amyloid PET scans (HC−Aβ). In LBD subjects, we compared the relationship between ^{18}F-flortaucipir retention and cerebrospinal fluid (CSF) tau, cognitive performance, and neuropathological tau at autopsy. The LBD cohort was stratified using an Aβ42 cut-off of 192 pg/mL to enrich for groups likely harboring tau pathology (LBD+Aβ = 11, LBD−Aβ = 9). ^{18}F-flortaucipir retention was higher in LBD+AB than HC−Aβ in five, largely temporal-parietal regions with sparing of medial temporal regions. Higher retention was associated with higher CSF total-tau levels (p = 0.04), poorer domain-specific cognitive performance (p = 0.02–0.04), and greater severity of neuropathological tau in corresponding regions. While ^{18}F-flortaucipir retention in LBD is intermediate between healthy controls and AD, retention relates to cognitive impairment, CSF total-tau, and neuropathological tau. Future work in larger autopsy-validated cohorts is needed to define LBD-specific tau biomarker profiles.

Current address of David G. Coughlin: Department of Neurosciences, University of California San Diego, La Jolla, CA, USA

David J. Irwin and Corey T. McMillan contributed equally to this article.

Role of the funding source: Avid Radiopharmaceuticals provided ^{18}F-flortaucipir tracer used in this study and were involved in the decision to publish the paper. They were not involved in study design, collection or data, analysis or interpretation of data, or the writing of this report.

* Corresponding author at: Department of Neurology, Hospital of the University of Pennsylvania, 3400 Spruce St, 3W Gates Building, Philadelphia, PA 19104, USA. Tel.: +215 614 0987; fax: +215 349 8464.

E-mail address: mcmillac@pennmedicine.upenn.edu (C.T. McMillan).

[1] Data used in preparation of this article were obtained from the Alzheimer's Disease Neuroimaging Initiative (ADNI) database (adni.loni.usc.edu). As such, the investigators within the ADNI contributed to the design and implementation of ADNI and/or provided data but did not participate in analysis or writing of this report. A complete listing of ADNI investigators can be found at: http://adni.loni.usc.edu/wp-content/uploads/how_to_apply/ADNI_Acknowledgement_List.pdf.

0197-4580/$ – see front matter © 2020 Elsevier Inc. All rights reserved.
https://doi.org/10.1016/j.neurobiolaging.2020.08.003

1. Introduction

Lewy body disorders (LBD)—dementia with Lewy bodies (DLB) and Parkinson's disease (PD)—are characterized pathologically by alpha-synuclein (SYN) inclusions in postmortem tissue; however, a significant proportion (>50%) of LBD patients have moderate to severe co-occurring Alzheimer's disease (AD) pathology (Aβ [amyloid beta] plaques and tau neurofibrillary tangles) sufficient for a secondary neuropathological diagnosis of AD (Irwin et al., 2017a). These levels of AD co-pathology are clinically relevant and associated with faster time to dementia, decreased overall survival (Irwin et al., 2017a; Jellinger et al., 2002), and contribute to specific cognitive and motor features in LBD (Coughlin et al., 2019a,b; Peavy et al., 2016). Molecular PET (positron emission tomography) imaging provides important in vivo information on the regional distribution of proteinopathies that otherwise has only previously been assessable at autopsy. ^{18}F-flortaucipir is a PET tracer with affinity for paired helical 33R/4R tau (Marquié et al., 2015) that shows increased retention in AD, with binding patterns consistent with pathologic distributions of tau in amnestic and non-amnestic variants (Nasrallah et al., 2018; Pontecorvo et al., 2017), and has recently been approved for use in evaluation for suspected AD based on postmortem studies (Fleisher et al., 2020) based on postmortem work but limited data exist in LBD. In LBD, paired helical 3R/4R tau accumulations are similar to that which is seen in AD (Iseki et al., 2003) and reports of ^{18}F-flortaucipir in LBD find increased retention in temporal, occipital, and parietal lobes, with lower standardized uptake value ratio (SUVR) values than typically seen in AD patients (Gomperts et al., 2016; Kantarci et al., 2017; Lee et al., 2018; Smith et al., 2018). In multimodal PET imaging studies, LBD patients with increased ^{18}F-flortaucipir often show evidence of co-occurring cerebral amyloidosis (Kantarci et al., 2017; Lee et al., 2018) but relationships between ^{18}F-flortaucipir retention and other biomarkers, including cerebrospinal fluid (CSF), are understudied.

We previously found that postmortem tau in LBD has a distinct regional distribution compared to AD, with relatively more tau present in temporal neocortex. Tau pathology was also associated with region-specific cognitive deficits across multiple domains (Coughlin et al., 2019a). Here we use a multimodal approach to examine in vivo tau biomarker profiles in a deeply phenotyped cohort of 20 LBD patients with ^{18}F-flortaucipir PET scanning, CSF sampling, and neuropsychological testing in close temporal proximity with the hypotheses that LBD patients with abnormal CSF Aβ would show regions of increased ^{18}F-flortaucipir compared to healthy controls and that ^{18}F-flortaucipir retention would correlate with CSF tau measures, region-specific neuropsychological performance, and neuropathological tau at autopsy.

2. Methods

2.1. Patients

Twenty patients with LBD (DLB: N = 15, PD-MCI [mild cognitive impairment]: N = 4, PDD: N = 1) were enrolled from the University of Pennsylvania's Movement Disorder Clinic, Frontotemporal Degeneration Center, and/or Alzheimer's Disease Core Center. All met clinical criteria for probable DLB (McKeith et al., 2017), PD-MCI (Litvan et al., 2011), or PDD (Emre et al., 2007). Five of 20 patients had ^{123}I-Ioflupane single-photon emission computed tomography scans, all of which showed evidence of dopamine transporter deficits. Additional 2 patients went to autopsy and had pathological confirmation of neocortical Lewy body disease. A local reference group of 15 healthy controls (HC-Aβ) who had undergone ^{18}F-flortaucipir PET scans was selected from the Penn Alzheimer's Disease Core Center Alzheimer's Disease Core Center who had (1) Mini-Mental State Examination (MMSE) or converted Montreal Cognitive Assessment scores ≥27 (Roalf et al., 2013), (2) negative amyloid PET scans (^{18}F-florbetaben, N = 13, ^{18}F-florbetapir, N = 2) determined by visual inspection by expert neuroradiologist (I.M.N.), and (3) had no history of neurologic or psychiatric disease. A disease reference group was obtained from the Alzheimer's Disease Neuroimaging Initiative (ADNI) database (adni.loni.usc.edu) (AD+Aβ: N = 12, MCI: N = 5, Dementia: N = 7). AD+Aβ cases were matched for age and cognitive impairment (assessed by MMSE) to the full LBD cohort (LBD−Aβ and LBD+Aβ together) and had positive ^{18}F-florbetapir PET scans with mean cortical SUVRs of >1.11 using a whole cerebellar reference (mean = 1.39, standard deviation [SD] = 0.14) using published methods (Landau et al., 2013). At the time when data were downloaded from the ADNI database, August 30, 2018, there were 41 individuals with a diagnosis of MCI or dementia, who had both a ^{18}F-flortaucipir PET scan and a positive florbetaben PET scan with mean cortical SUVR >1.11 (Jagust et al., 2015). From that cohort, ADNI cases with greater age and lower MMSE were sequentially removed for the matching process until the ADNI cohort had group average MMSE and age at PET scan that was statistically similar to the LBD cohort (see Supplemental figure for flow chart of case selection). Data used in the preparation of this article were obtained from the ADNI database (adni.loni.usc.edu). The ADNI was launched in 2003 as a public-private partnership, led by Principal Investigator Michael W. Weiner, MD. The primary goal of ADNI has been to test whether serial magnetic resonance imaging (MRI), PET, other biological markers, and clinical and neuropsychological assessment can be combined to measure the progression of MCI and early AD. All subjects provided written informed consent and all study procedures were approved by the University of Pennsylvania's Institutional Review Board.

2.2. Neuroimaging

2.2.1. Magnetic resonance imaging

T1-weighted MR images for LBD and HC-Aβ participants were acquired axially with 0.98 mm × 0.98 mm × 1 mm voxels, a 256 × 192 matrix, repetition time of 1620 ms, inversion time of 950 ms, and a flip angle of 15° on a 3T Siemens scanner. Scans were visually inspected for quality (J.S.P. and E.R.) to rule out motion artifact or other distortions. Advanced Normalization Tools (ANTs) (Avants et al., 2011) was used to process and symmetrically and diffeomorphically register each image to a healthy control template (Klein et al., 2017; McMillan and Wolk, 2016). We used a joint label fusion approach to align the Mindboggle-101 "Brain Color" labels (based on the Desikan-Killiany-Tourville label scheme) with each image using pseudo-geodesic registration (Wang et al., 2013).

2.2.2. ^{18}F-flortaucipir PET scans

LBD and HC-Aβ scans were performed on a Phillips Ingenuity TF PET scanner. About 6 × 5 minute frames were acquired 75–105 minutes after injection of approximately 10 mCi of ^{18}F-flortaucipir. AD+Aβ cases were acquired on a variety of scanners using similar protocols (Jagust et al., 2015; Weiner et al., 2017). Regional SUVR was assessed using Mindboggle-101 "Brain Color" labels (Klein and Tourville, 2012), with cerebellar gray matter reference after partial volume correction (PVC) using the reblurred Van-Cittert method (Thomas et al., 2016). PVC data were highly correlated with non-corrected data ($R^2 = 0.98$, $p < 0.001$). Regional SUVR measurements were averaged across hemispheres for leaving 58 regions for comparison. PVC and non-PVC values for the hippocampus were significantly correlated ($R^2 = 0.97$, $\beta = 0.99$, $t(46) = 40.7$, $p < 0.001$). Baker et al. (2019) suggested that PVC alone may not be sufficient to account for off-target binding effects in the hippocampus. To further address this issue, we conducted a

supplementary analysis examining hippocampal signal independent of tracer uptake in the choroid plexus, thalamus, and putamen, which are known sources of off-target binding (Baker et al., 2019). The choroid plexus was localized using the corresponding label from the aparc.a2009s+aseg parcellation image generated by the FreeSurfer recon-all pipeline. We then removed voxels that overlapped with this structure from the BrainColor labels used in the main analysis and performed PVC on the modified labels using the geometric transfer matrix method (Rousset et al., 1998; Thomas et al., 2016). From the hippocampal signal we subtracted SUVRs in the thalamus, putamen, and choroid plexus, weighted by the regression coefficients for Braak stage II regions calculated by Baker et al. (2019) in their analysis of amyloid-negative control participants. This procedure yielded an estimate of hippocampal retention independent of known markers of off-target binding.

2.3. Cerebrospinal fluid measurements

CSF Aβ42, p-tau, and t-tau were acquired using ADNI standard operating procedures and analyzed using a Luminex platform and AlzBio3 immunoassay reagents (AlzBio3; Innogenetics NV, Gent, Belgium), as previously reported (Irwin et al., 2018). Median time between CSF sampling and ^{18}F-flortaucipir scanning was 58 days (interquartile range: 28–217 days). We used an established biomarker independent of tau, CSF Aβ42, to divide the LBD cohort into those likely harboring cerebral amyloidosis (LBD+Aβ, Aβ42 ≤192 pg/mL, N = 11) and those unlikely to have cerebral amyloidosis (LBD−Aβ, Aβ42 >192 pg/mL, N = 9) (Shaw et al., 2009).

2.4. Neuropathology

As of May 16, 2019, 2 LBD subjects had died and participated in brain donation. Autopsies were performed at the Penn Center for Neurodegenerative Disease Research using validated neuropathological criteria (McKeith et al., 2017; Montine et al., 2012). Tissue was fixed overnight in 10% neutral-buffered formalin processed, and immunohistochemically using described procedures (Irwin et al., 2016b; Toledo et al., 2014). Expert neuropathologists (E.B.L., J.Q.T.) applied current diagnostic criteria and assigned Thal phases, Braak tau stages, CERAD neuritic plaque stages (Montine et al., 2012), and SYN Lewy body stages (McKeith et al., 2017). Sections were immunostained for tau (AT8; Thermo-Scientific), Aβ (NAB228; Santa-Cruz), and SYN (MJF-R13; Abcam) for digital pathology experiments. Images of histology slides at 20× magnification were obtained using a Lamina slide scanning system (Perkin Elmer, Waltham MA) and Halo digital image software v1.90 (Indica Labs, Albuquerque, NM) calculated %area occupied (%AO) of reactivity for tau, Aβ, and SYN in regions of interest after color deconvolution intensity thresholds were optimized for each stain as previously published (Coughlin et al., 2019a; Irwin et al., 2016b). We also performed an analysis using object detection to detect %AO of tau tangles alone (Irwin et al., 2016b).

2.5. Neuropsychological testing

Neuropsychological testing was administered by trained research personnel (Watson et al., 2013) near the time of ^{18}F-flortaucipir PET (median time from testing to PET: 41 days; interquartile range: 9–100 days) including MMSE, clinical dementia rating scale sum of boxes (CDR-SOB), multi-lingual naming test (MINT), letter fluency (F-words), Benson figure copy, and delayed recall (Beekly et al., 2007).

2.6. Statistical analysis

Demographic differences were assessed using chi-squared test, Fisher's exact test, or analysis of variance as appropriate. ^{18}F-flortaucipir mean cortical SUVR and regional SUVR, which were averaged across hemispheres, were compared across groups using linear regression controlling for age and sex. Regional SUVR analysis used the prespecified threshold of $p = 0.01$ for significance. Neuropsychological performance was compared to regional SUVR values in prespecified targeted analyses using linear regression also controlling for age and sex. Specifically, MMSE and CDR-SOB, which are global measures of cognition, were compared to mean cortical SUVR and the composite value derived from Braak Tau associated regions. MINT tests naming associated with left temporal cortex function and therefore was compared to left middle temporal gyrus retention (Abel et al., 2015; Emerton et al., 2014; Hamberger et al., 2003, 2016). Letter fluency is a frontally mediated cognitive task and was compared to middle frontal gyrus retention (Baldo and Shimamura, 1998; Moscovitch, 1994; Quinn et al., 2012). Benson figure copy is a parietal lobe-mediated visuospatial task that was compared to right angular gyrus retention (Chen et al., 2016; Han et al., 2015), and Benson figure recall relies on medial temporal process so was compared to hippocampus retention (PVC and non-PVC values) (McConley et al., 2008; Xu et al., 2019; Zammit et al., 2017a,b).

Mean cortical SUVR was compared to natural log transformed values of CSF Aβ42, t-tau, and p-tau using linear regression adjusting for age and sex. Because the use of cortical SUVR values may obscure meaningful analyses of regions with elevated tau pathology, we also compared CSF measurements to a composite measure of the average SUVR values of regions with significantly higher retention in LBD over HC-Aβ as well as a composite measure average SUVR regions implicated in traditional Braak tau staging (hippocampus, entorhinal cortex, inferior temporal gyrus, middle temporal gyrus, angular gyrus, middle frontal gyrus, and calcarine cortex). Subanalyses were performed after the removal of outlier values defined as greater than ±2 SD from the mean. $p < 0.05$ was observed as the statistical threshold for the hypothesis-driven CSF and neuropsychological analyses. Statistical analysis was performed using STATA v15.1 (College Station, TX, USA). All procedures were performed under protocols approved by the University of Pennsylvania Institutional Review Board.

3. Results

3.1. Patient characteristics

Patient characteristics are described in Table 1. There were more female participants in the AD+Aβ and HC−Aβ group than in the LBD cohort ($\chi^2(1) = 11.5, 5.8, p = 0.001, 0.03$ respectively), and therefore we covary for sex in all subsequent analyses. LBD+Aβ participants performed worse than LBD−Aβ on MMSE testing ($t(18) = 2.4$, $p = 0.03$) and had fewer years of education ($t(18) = 3.4$, $p = 0.004$) but otherwise there were no differences in characteristics. There were no significant differences in age at PET scan or MMSE testing between AD+Aβ and the full LBD cohort as designed.

3.2. Comparative ^{18}F-flortaucipir retention

Group ^{18}F-flortaucipir retention patterns in HC-Aβ, LBD, and AD+Aβ are shown in Fig. 1 and individual values are shown in Fig. 2. The total LBD group showed mild ^{18}F-flortaucipir retention in posterior temporal-parietal regions with total SUVR significantly elevated compared to HC−Aβ (HC−Aβ mean cortical SUVR 1.09, SD 0.07; LBD total cohort mean cortical SUVR 1.16, SD 0.12; $\beta = 0.43$, $t(34) = 2.3$, $p = 0.03$). Next, we examined biomarker-defined

Table 1
Patient demographics

	HC−Aβ (n = 15)	LBD total (n = 20)	LBD−Aβ (n = 9)	LBD+Aβ (n = 11)	AD+Aβ (n = 12)
Clinical phenotype, count	NA	DLB: 15 PD-MCI: 4 PDD: 1	DLB: 6 PD-MCI: 3	DLB: 9 PD-MCI: 1 PDD: 1	Dementia: 7 MCI: 5
Sex[a], count	Male: 8 Female: 7	Male: 17 Female: 3	Male: 7 Female: 2	Male: 10 Female: 1	Male: 3 Female: 9
Race, count	White: 13 Black: 2	White: 20	White: 9	White:11	White:12
Age of onset	NA	62.8 (6.2)	61.7 (6.4)	63.6 (6.3)	62.0 (9.2)
Disease duration at scan[b]	NA	5.4 (3.5)	6.2 (3.0)	3.9 (2.9)	9 (4.9)
Age at scan	72.7 (6.0)	67.7 (5.6)	67.9 (6.6)	67.5 (4.9)	71.4 (5.9)
Education[c]	14.5 (3.1)	15.7 (2.5)	17.3 (1.7)	14.3 (2.3)	15.9 (3.0)
MMSE[d,e]	29.3 (0.9)	27.0 (2.7)	28.4 (1.1)	25.8 (3.1)	24.3 (5.6)
CDR-sum of boxes[f]	0 (0)	N = 15 4.87 (2.8)	N = 7 3.64 (1.5)	N = 8 5.94 (3.4)	4.25 (3.1)

Data shown are mean (standard deviation) from the entirety of the group unless otherwise specified. There were no significant differences in age at scan, MMSE, or CDR-sum of boxes between the AD+Aβ group and the LBD total cohort. If an MoCA was performed closer to PET scan, MoCA score was converted to equivalent MMSE score.
Key: Aβ, amyloid beta; AD, Alzheimer's disease; ANNOVA, analysis of variance; CDR, clinical dementia rating; DLB, dementia with Lewy bodies; HC, healthy controls; LBD, Lewy body disorders; MCI, mild cognitive impairment; MMSE, Mini-Mental State Examination; MoCA, Montreal Cognitive Assessment; NA, not applicable; PD, Parkinson's disease; PET, positron emission tomography.
[a] Fisher's exact chi-squared test, $p = 0.005$.
[b] Time from MCI onset used for AD+Aβ.
[c] ANOVA $F(3,43) = 3.0$, $p = 0.04$.
[d] MMSE closest to PET scan was assessed.
[e] ANOVA $F(3,43) = 6.1$, $p = 0.002$.
[f] ANOVA $F(3,37) = 10.7$, $p < 0.001$.

subgroups of LBD and found higher total mean cortical ^{18}F-flortaucipir SUVR in LBD+Aβ relative to HC−Aβ (LBD+Aβ mean cortical SUVR 1.19, SD 0.15; $\beta = 0.55$, $t(25) = 2.4$, $p = 0.02$) and only a trend toward significance between LBD−Aβ and HC−Aβ (LBD-Aβ mean cortical SUVR 1.11, SD 0.06, $p = 0.07$). We observed 2 cases with high SUVR in the LBD+Aβ group; when these cases were removed from analysis, there was still significantly higher mean cortical SUVR in LBD+Aβ over HC−Aβ ($\beta = 0.53$, $t(23) = 2.5$, $p = 0.02$). In regional analyses, ^{18}F-flortaucipir retention was higher in LBD+Aβ than HC−Aβ in 5 regions (angular gyrus, lingual gyrus, calcarine cortex, occipital fusiform gyrus, middle frontal gyrus; $p < 0.01$) and did not show increased retention in the medial temporal areas (see Fig. 3; similar results were observed without hemispheric averaging, Supplemental Table 1). LBD-Aβ had higher uptake than HC−Aβ in the superior frontal gyrus alone ($p = 0.002$). In the matched AD+Aβ group, we found higher mean cortical ^{18}F-flortaucipir retention (AD+Aβ mean cortical SUVR 1.40, SD 0.42; $\beta = 0.24$, $t(26) = 2.4$, $p = 0.03$) and regionally higher retention in 6 regions (angular gyrus, basal forebrain, entorhinal cortex, fusiform gyrus, hippocampus, parahippocampal gyrus) compared to HC−Aβ (Fig. 4). The AD+Aβ group had similar average cortical ^{18}F-flortaucipir SUVR to LBD patients (vs. LBD−Aβ: $p = 0.20$ and vs. LBD+Aβ: $p = 0.40$). AD+Aβ had significantly higher unadjusted hippocampal retention (mean SUVR 1.46, SD 0.25) than LBD+Aβ and trended toward increase over LBD−Aβ (vs. LBD+Aβ: mean SUVR 1.15, SD 0.11, $p = 0.008$ and vs. LBD−Aβ: mean SUVR 1.15, SD 0.19, $p = 0.07$) (Fig. 4). We did not observe any regions of higher retention in LBD+Aβ than AD+Aβ, LBD−Aβ than LBD+Aβ or AD+Aβ, or in HC−Aβ relative to AD+Aβ, LBD+Aβ, or LBD−Aβ.

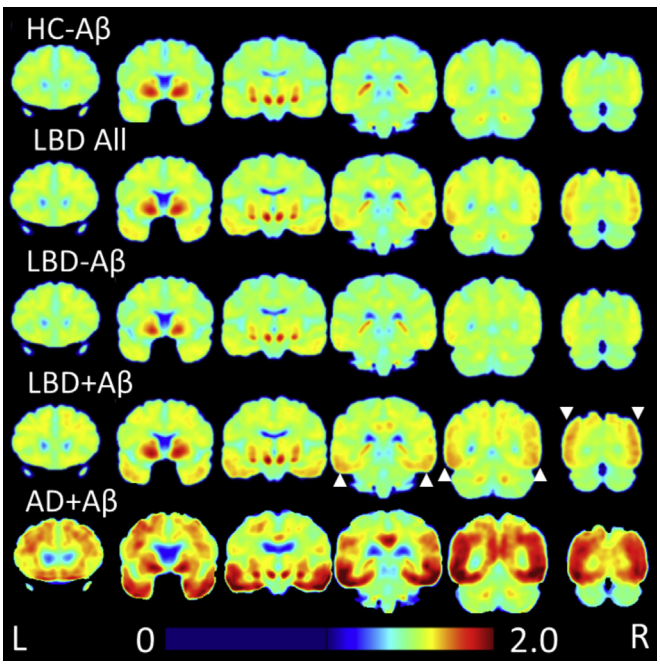

Fig. 1. Heatmap of ^{18}F-flortaucipir retention; average ^{18}F-flortaucipir uptake for each group is shown in coronal sections. LBD+Aβ has higher uptake than HC−Aβ in posterior regions, indicated by white arrows. LBD−Aβ is very similar to HC−Aβ. LBD uptake in both LBD−Aβ and LBD+Aβ is less than AD+Aβ. Abbreviations: Aβ, amyloid beta; AD, Alzheimer's disease; HC, healthy controls; LBD, Lewy body disorders.

Regarding the hippocampus specifically, when using the methods described in Baker et al., (2019) was utilized to account for off-target choroid plexus binding, AD+Aβ had higher hippocampal retention than both LBD−Aβ and LBD+Aβ (AD+Aβ mean 1.31, SD 0.23 vs. LBD−Aβ mean 0.96, SD 0.17, $p = 0.02$ and vs. LBD-Aβ mean 0.95, SD 0.10, $p = 0.001$) (Baker et al., 2019) ($\beta = 0.33$, $t(20) = 2.7$, $p = 0.02$) (see Supplemental Table 2). Although there was a modest but significant correlation between choroid plexus and hippocampal retention using non-PVC values ($R^2 = 0.06$, $p = 0.02$), this was not observed when PVC was employed ($R^2 = 0.01$, $p = 0.27$). There were no differences in choroid plexus binding between groups using either non-PVC or off-target corrected values (Supplemental Table 3).

3.3. In vivo tau and neuropsychological performance

In domain-specific analyses within the LBD cohort, reduced MINT confrontation naming was inversely related to increased left middle temporal gyrus retention ($\beta = -0.45$, $t(19) = -2.14$, $p <$

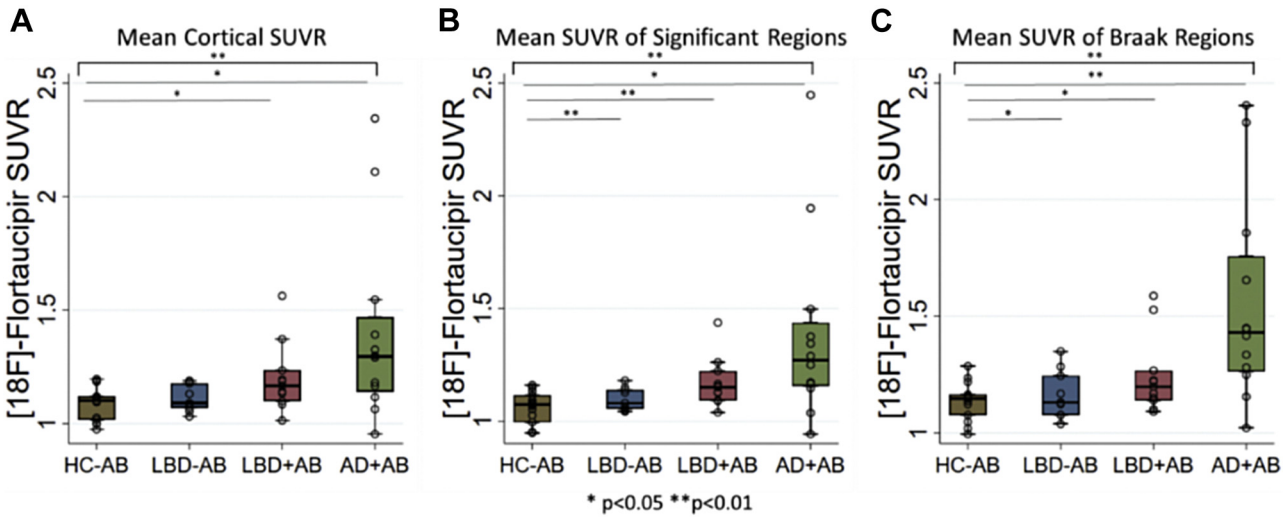

Fig. 2. ^{18}F-flortaucipir retention values. Boxplots depict median, interquartile range, and range of 18F-flortaucipir retention for (A) average cortical regions, (B) average SUVR from those regions with elevated retention in LBD versus healthy controls, and (C) average SUVR from regions associated with traditional Braak tau staging. Brackets indicate ANOVA results while lines indicate significant differences between groups. $^{*}p < 0.05$, $^{**}p < 0.01$. Abbreviations: ANOVA, analysis of variance; LBD, Lewy body disorders.

0.05). Additionally, reduced performance on the Benson figure copy was inversely related to increased right angular gyrus retention ($\beta = -0.52$, $t\,(19) = -2.61$, $p = 0.02$). We observed a trend toward increased mean cortical ^{18}F-flortaucipir retention with increased CDR-SOB ($\beta = 0.51$, $t\,(14) = 1.96$, $p = 0.08$) and a significant association of ^{18}F-flortaucipir retention in the Braak tau pathology associated regions and CDR-SOB scores ($\beta = 0.71$, $t\,(14) = 3.10$, $p = 0.01$). We did not find associations of mean cortical retention and MMSE, letter fluency and middle frontal gyri retention or between Benson figure delayed recall and hippocampal retention ($p > 0.05$ with either PVC or non-PVC values).

3.4. ^{18}F-flortaucipir retention and CSF tau biomarkers

In the LBD cohort elevated mean cortical ^{18}F-flortaucipir uptake was associated with increased CSF t-tau levels ($\beta = 0.40$, $t\,(19) = 2.2$, $p = 0.045$), but was not with CSF p-tau ($\beta = 0.28$, $t\,(19) = 1.3$, $p = 0.20$). Increased ^{18}F-flortaucipir retention was inversely associated with CSF Aβ42 ($\beta = -0.59$, $t\,(19) = -2.9$, $p = 0.01$) (Fig. 5). Next, because total SUVR values may obscure associations with focal regions of retention, we performed a focused analysis using the average SUVR values of the 6 regions with elevated retention in LBD over HC−Aβ and observed similar associations (t-tau: β =

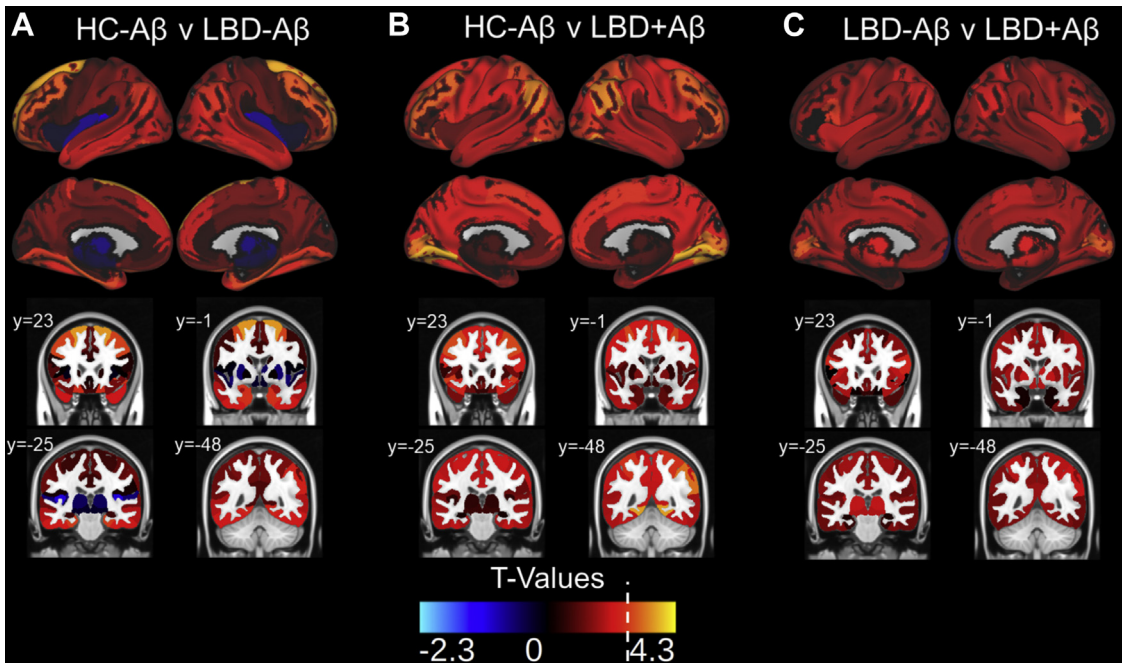

Fig. 3. ^{18}F-flortaucipir retention patterns in LBD versus HC-Aβ; surface projections and representative coronal sections show *t*-values associated with the following comparisons in each region of interest: (A) HC−Aβ versus LBD−Aβ, (B) HC−Aβ versus LBD+Aβ, and (C) LBD−Aβ versus LBD+Aβ, with positive *t*-values corresponding the latter group in each comparison. LBD+Aβ has increased uptake over HC−Aβ in frontal, parietal, temporal, and occipital regions with relative sparing of the medial temporal lobes. The white broken line on the *t*-value color scale indicated the *t*-value relating to $p = 0.01$. No negative *t*-values reached significance. Example coronal slices show regional *t*-values projected onto the standardized brain atlas derived from Montreal Neurological Institute (MNI) with labeled *y*-axis coordinates. Abbreviations: Aβ, amyloid beta; HC, healthy controls; LBD, Lewy body disorders.

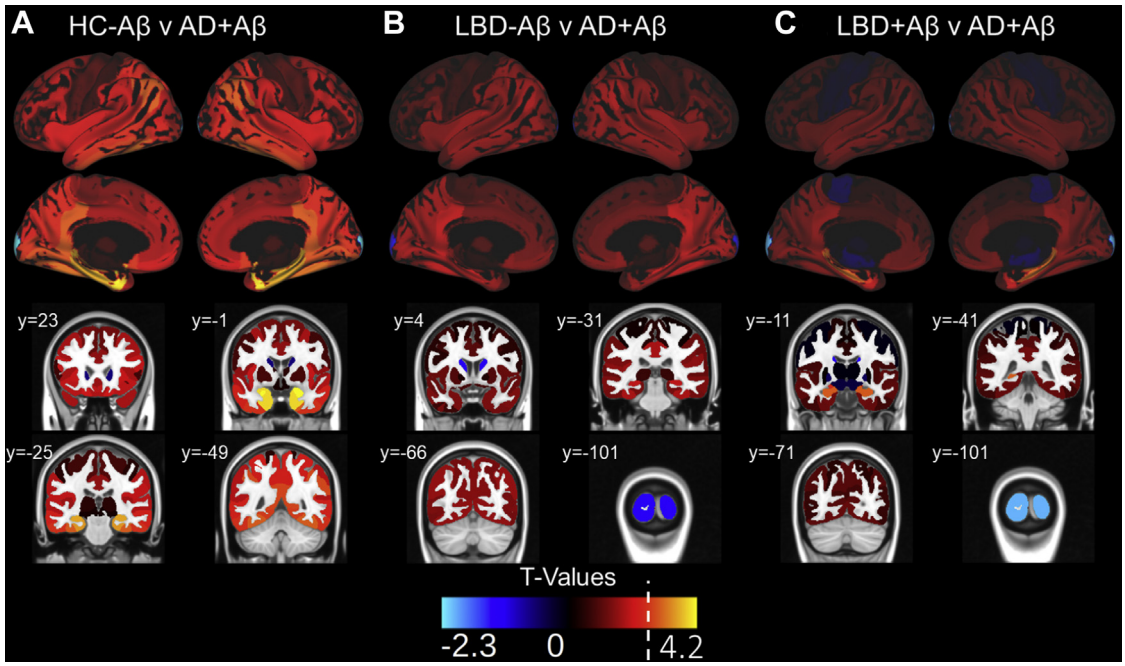

Fig. 4. ^{18}F-flortaucipir retention patterns in AD+Aβ versus HC−Aβ and LBD. Surface projections and representative coronal sections show *t*-values associated with the following comparisons in each region of interest: (A) HC−Aβ versus AD+Aβ, (B) LBD−Aβ versus AD+Aβ, and (C) LBD+Aβ versus AD+Aβ with positive *t*-values corresponding to the latter group in the comparison. AD+Aβ has increased uptake over HC−Aβ in medial temporal lobe areas as well as temporal, frontal, and parietal regions. AD+Aβ has higher uptake than LBD in the hippocampus. A white line on the *t*-value scale marks the level corresponding to $p = 0.01$ in this analysis. No negative *t*-values reached significance. Example coronal slices show regional *t*-values projected onto the standardized brain atlas derived from Montreal Neurological Institute (MNI) with labeled *y*-axis coordinates. Abbreviations: Aβ, amyloid beta; AD, Alzheimer's disease; HC, healthy controls; LBD, Lewy body disorders.

0.41, t (19) = 2.2, $p = 0.04$; p-tau: β = 0.29, t (19) = 1.3, $p = 0.2$; Aβ42: β = −0.56, t (19) = −2.6, $p = 0.02$). Finally, we tested the association of CSF and ^{18}F-flortaucipir retention in the LBD+Aβ subgroup alone and found associations in t-tau (β = 0.63, t (10) = 2.8, $p = 0.03$), but not p-tau (β = 0.37, t (10) = 1.2, $p = 0.3$) or Aβ42 (β = −0.61, t (10) = −2.1, $p = 0.08$). To exclude the possibility that outlier cases with high ^{18}F-flortaucipir or CSF values are driving these associations, we performed similar analyses after excluding data greater than ±2.0 SD from the mean of each and found similar results (t-tau: β = 0.62, t (17) = 2.7, $p = 0.02$; p-tau: β = 0.50, t (17) = 1.8, $p = 0.09$; Aβ42: β = −0.68, t (16) = −2.8, $p = 0.02$). We additionally observed similar associations when comparing SUVR values from regions implicated in traditional Braak tau staging (t-tau: β = 0.48, t (19) = 2.7, $p = 0.02$; p-tau: β = 0.37, t (19) = 1.77, p = 0.10; Aβ42: β = −0.66, t (19) = −3.31, $p = 0.004$).

3.5. ^{18}F-flortaucipir retention and neuropathologic tau

Both autopsy cases had diffuse/neocortical Lewy body pathology (McKeith et al., 2017). β-amyloid Thal phasing and CERAD scoring are found in Fig. 6. Case 1 had neurofibrillary tau restricted to the hippocampal cornu ammonis and entorhinal cortex (Braak stage II: B1) with mean cortical ^{18}F-flortaucipir SUVR of 1.05. Case 2 had neurofibrillary tau pathology in the gray matter of limbic and all neocortical areas except visual cortex (Braak stage V: B3) with mean cortical ^{18}F-flortaucipir uptake of 1.48. Digital histological measurements showed that regions with higher total tau% AO and higher neurofibrillary tangle%AO generally had higher ^{18}F-flortaucipir retention, whereas such patterns were not observed for Aβ or SYN.

4. Discussion

We examined ^{18}F-flortaucipir retention patterns in LBD patients with cognitive impairment compared to amyloid PET-negative healthy controls and amyloid PET-positive AD patients from the ADNI study matched on age and cognitive impairment. This is a unique multimodal study of ^{18}F-flortaucipir PET imaging, biofluid tau markers, and neuropathological tau in LBD. We find several regions of increased ^{18}F-flortaucipir retention in LBD patients with CSF measurements consistent with cerebral amyloidosis (LBD+Aβ) while LBD patients with normal CSF measurements (LBD−Aβ) had fewer compared to healthy controls. Areas of increased retention were of intermediate degree and largely in temporal, parietal, and occipital lobes with sparing of medial temporal lobe structures, which are more heavily affected in AD. ^{18}F-flortaucipir retention correlated with region-specific cognitive measures, suggesting that tau pathology in LBD is clinically relevant. There were moderate correlations of global and regional SUVR with CSF t-tau levels and in 2 autopsy cases, regional neuropathological tau burden measured by digital histology appeared to be higher in areas with increased ^{18}F-flortaucipir retention. These data provide novel insights into the in vivo clinical correlates of tau pathology in LBD, and while the clinical utility of ^{18}F-flortaucipir remains to be determined, our observations have important research implications for the biomarker classification of LBD patients.

Although it has recently been established that ^{18}F-Flortaucipir retention relates to neuropathological deposition of tau in AD (Fleisher et al., 2020), its use in other disease states is still investigational (Ossenkoppele et al., 2018; Tsai et al., 2019; Whitwell et al., 2017, 2020). Previous investigations of ^{18}F-flortaupcipir in LBD show retention values that are typically intermediate between healthy controls and AD with retention being most commonly elevated in temporo-parietal regions (Gomperts et al., 2016;

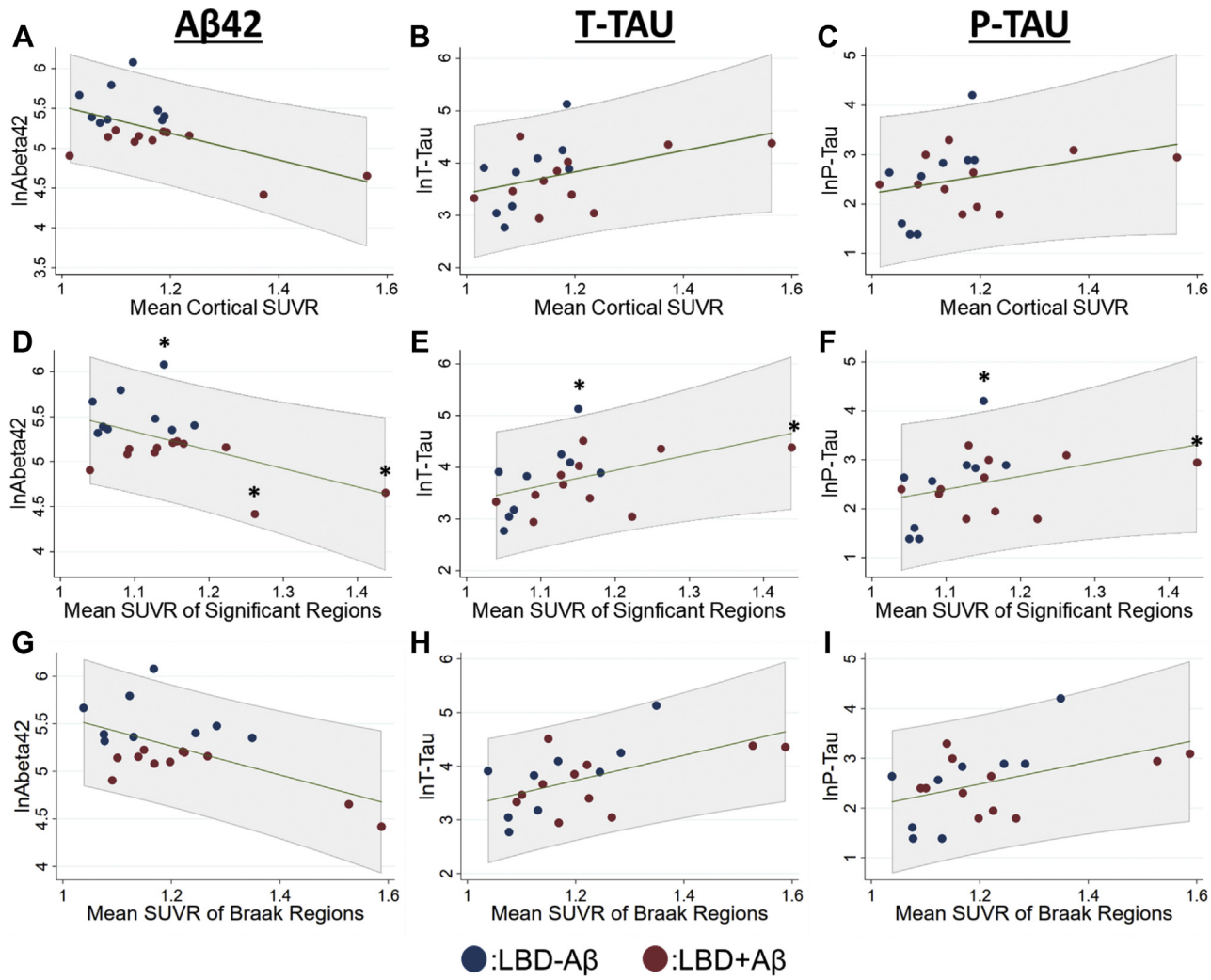

Fig. 5. Relationship of CSF measurements to ^{18}F-flortaucipir Retention in LBD. (A-C) Scatterplots showing relationship between mean cortical ^{18}F-flortaucipir retention; (D-F) average ^{18}F-flortaucipir retention in the 6 regions with elevations in LBD compared to HC−Aβ; (G-I) average ^{18}F-flortaucipir retention in regions implicated in traditional Braak tau staging, and log transformed values of CSF Aβ42, t-tau, and p-tau. Linear prediction is shown in green with 95% confidence intervals shown in gray shaded region. We performed similar models after excluding data greater than ± 2.0 SD from the mean of CSF or PET data (marked by asterisks). Abbreviations: Aβ, amyloid beta; CSF, cerebrospinal fluid; HC, healthy controls; LBD, Lewy body disorders; PET, positron emission tomography.

Kantarci et al., 2017; Lee et al., 2018; Smith et al., 2018). We similarly found that temporo-parietal and occipital regions in the LBD+Aβ cohort exhibited increased ^{18}F-flortaucipir retention in our data-driven approach to selecting LBD-specific regions for further correlative analyses with CSF markers. Additionally, these findings mirror our recent digital histology postmortem work where LBD patients with moderate/severe levels of AD neuropathologic change showed intermediate density of tau pathology compared with AD with relatively increased concentrations in the temporal lobe (Coughlin et al., 2019a). Since standard neuropathological sampling is relatively sparse compared to whole-brain in vivo analyses, there is scant histopathological data to further guide the definition of LBD-associated regions for tau uptake. Future work in larger datasets will examine the relationship between CSF tau analytes and regional distribution of tau between AD and LBD-associated cortical regions. It is important to note that patients with PD and PD-MCI are most frequently cited as having similar ^{18}F-flortaucipir retention as healthy controls and only some of those with PDD and DLB have elevated retention (Gomperts et al., 2016; Hansen et al., 2017; Kantarci et al., 2017; Lee et al., 2018; Winer et al., 2018). This is not unexpected given the known associations of greater likelihood of more significant tau burdens in PDD and DLB (Coughlin et al., 2019b; Irwin et al., 2017a). Thus, the use of ^{18}F-flortaucipir in LBD may be relegated to detection of co-pathology in patients with cognitive impairment, such as the subjects included in this study. In this study, we employed a novel biomarker classification approach using a CSF Aβ42 cut point to enrich the LBD+Aβ group for cases likely harboring tau pathology. Although our approach to use CSF delineation is unique, others have used amyloid-PET in a similar manner and found that most (Lee et al., 2018), but not all (Gomperts et al., 2016; Kantarci et al., 2017) LBD patients with positive amyloid-PET scans also have increased ^{18}F-flortaupcipir retention. It is unclear if this dissonance is due to decreased sensitivity of amyloid-PET for diffuse plaques (Burack et al., 2010) commonly seen in LBD, or if tau deposition could occur independently of amyloidosis in LBD. Further longitudinal work is needed to resolve the dynamic profiles of tau and Aβ in LBD. Our study, in contrast to previous, uses biomarker-defined reference cohorts and matching of an AD group by cognitive impairment in an attempt to control for disease severity, which may explain the more modest differences between the AD+Aβ group versus LBD patients documented elsewhere.

A Neuropathologic and PET Characteristics

	Months from PET to Autopsy	Thal Phase	Braak Tau	CERAD Stage	McKeith LB Stage	Mean ^{18}F-Flortaucipir Uptake
Case 1	5	A2	B1	C1	Neocortical	1.05
Case 2	8	A3	B3	C3	Neocortical	1.48

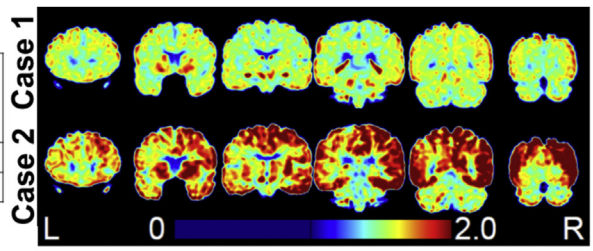

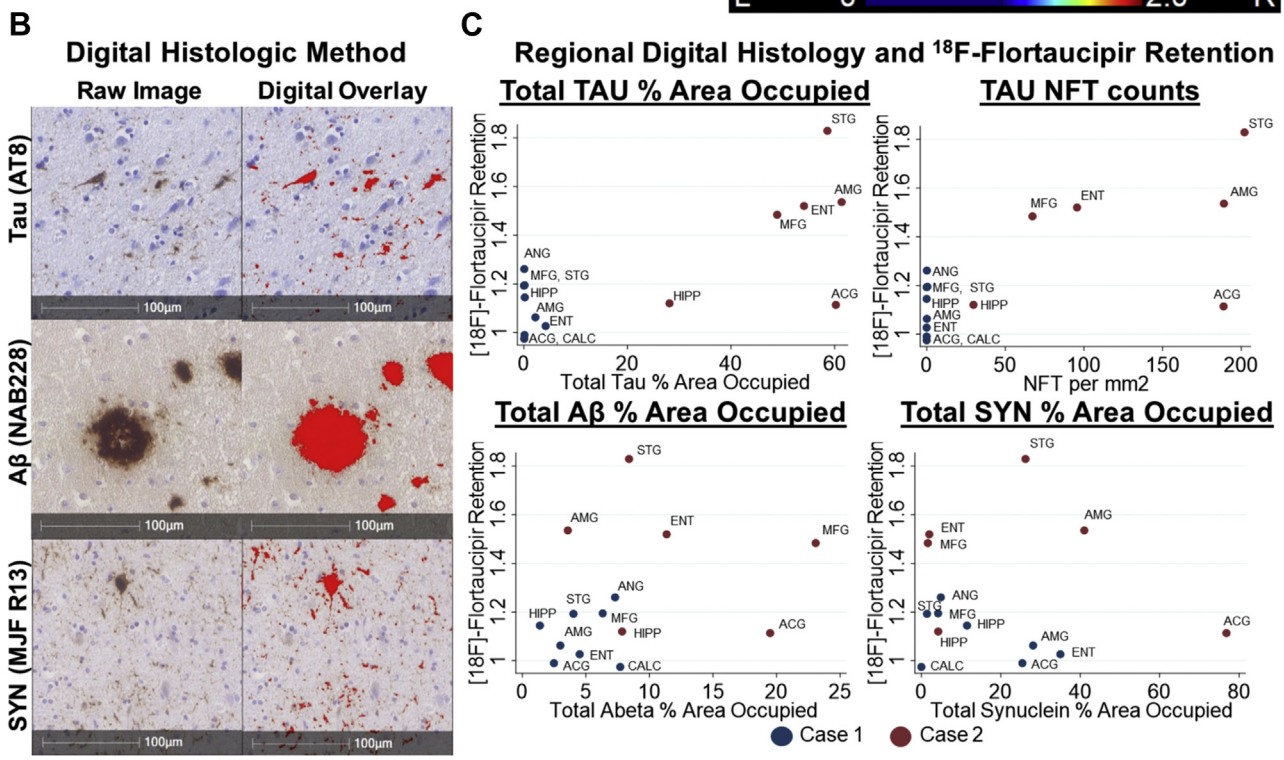

Fig. 6. Relationships between ^{18}F-flortaucipir retention and neuropathology. (A) Neuropathologic characteristics and staging for tau, Aβ, and synuclein pathology and coronal images from ^{18}F-flortaucipir PET scans from each case. (B) Representative images of slides stained for tau (AT8), Aβ (Nab228), and SYN (MJF R13) and the digital overlay of the detection algorithms used to generate % area occupied values. (C) Relationship between ^{18}F-flortaucipir retention and % area occupied of for tau (AT8), Aβ (NAB228), and SYN (MJF R-13). Tau was additionally assessed by neurofibrillary tangle counts per mm^2. Abbreviations: Aβ, amyloid beta; ACG, anterior cingulate gyrus; AMG, amygdala; ANG, angular gyrus; CALC, calcarine cortex; ENT, entorhinal cortex; HIPP, hippocampus; NFT, neurofibrillary tangle; MFG, mid frontal gyrus; STG, superior temporal gyrus.

In LBD, AD co-pathology is related to decreased survival (Coughlin et al., 2019b; Irwin et al., 2012, Irwin et al., 2017a; Jellinger et al., 2002; Wakisaka et al., 2003) and to specific cognitive and motor features (Coughlin et al., 2019a,b; Jellinger et al., 2002; Kraybill et al., 2005; Peavy et al., 2016). Confrontation naming has been previously linked to AD co-pathology in LBD (Coughlin et al., 2019a; Peavy et al., 2016) and visuospatial dysfunction is considered a core clinical feature of dementia in LBD (Emre et al., 2007; McKeith et al., 2017). In DLB, higher levels of tau pathology are associated with a lower likelihood of visual hallucinations and cognitive fluctuations, which has led to the incorporation of tau pathology into the neuropathological assessment of DLB (McKeith et al., 2005). In our recent study using digital histologic methods in LBD with dementia, we found that pathologic tau was the strongest correlate of global and domain-specific cognitive dysfunction (Coughlin et al., 2019a). Here we find that regional ^{18}F-flortaupcipir retention correlated with domain-specific measures of cognition, including confrontation naming with temporal lobe retention and visuospatial functioning with angular gyrus retention. A prior study in LBD found parietal lobe retention associated with verbal fluency (Smith et al., 2018). We did not find an association of hippocampal SUVR and episodic memory, which may be due to sample size, heterogeneity, or imaging methods in this initial report. These findings add to the growing literature of detrimental influence of tau co-pathology on cognition in LBD.

We find here novel evidence for higher ^{18}F-flortaucipir retention in LBD patients with an amyloid CSF biomarker profile. The interpretation of AD CSF biomarkers in LBD is not fully clear and, in some instances low CSF Aβ may be associated with pure synucleinopathy without postmortem plaques (Irwin et al., 2018). Our group previously found an association of CSF t-tau, but not p-tau with postmortem tau pathology in autopsy-confirmed LBD patients (Irwin et al., 2018). The relationship between CSF tau and ^{18}F-flortaucipir imaging in LBD is understudied, although an association has been suggested in AD (La Joie et al., 2018; Mattsson et al., 2018). We find novel evidence for a potential linear relationship of CSF t-tau levels but not p-tau with ^{18}F-flortaucipir retention. The distinction between CSF t-tau and p-tau in LBD may be due to methodological issues with CSF assays and further work is needed to fully resolve the relationship between these biomarkers in LBD.

In the 2 patients with autopsies we found higher mean cortical SUVR in the patient with advanced Braak tau stage V (1.48) compared to the patient with low level Braak tau stage II (1.05). Using digital analysis we found overall greater regional microscopic

tau pathology in postmortem tissue obtained from regional measurements of higher ^{18}F-flortaucipir retention during life, as have others (Lowe et al., 2019). There was some discrepancies in the anterior cingulate cortex of case 2, which had low retention despite high tau burden. Region-specific areas of the brain may have different retention rates. Regional standardization, while beyond the scope of the current study, may resolve these discrepancies (Vemuri et al., 2017). It remains to be determined whether ^{18}F-flortaucipir provides a continuous marker of tau severity or a categorical marker. Indeed, a recent clinicopathological study suggested that visual reads have a high sensitivity and specificity for B3 pathology, but quantitative SUVR analyses were only exploratory (Fleisher et al., 2020). Likewise, while amyloid approaches like florbetapir are typically also interpreted categorically based on validated visual reads (Clark et al., 2012), there is mounting evidence that continuous measurements of sub-threshold amyloid may have clinical utility (McMillan and Chételat, 2018). Thus, while 2 cases in our series appear to have categorically elevated ^{18}F-flortaucipir retention relative to the remainder of the cohort, our continuous analyses excluding these cases still appears to support a linear association between ^{18}F-flortaucipir tau measurements of tau load and clinical features of LBD (Fig. 4).

There are limitations to this study. Although we had rare multimodal in vivo imaging and biofluid assessments and used a unique biomarker-based approach to classify subjects, we had relatively small numbers of participants which limited complex statistical modeling. Not all of the LBD participants had dopamine transporter single-photon emission computed tomography scans or autopsies to aid in the confirmation clinical diagnosis; however, the criteria of probable PD and DLB are currently felt to be highly specific (Rizzo et al., 2018, 2016). We used AD+Aβ patients from the ADNI study, which introduces variability in imaging protocols. In spite of this variability, we found biologically relevant regional elevations in AD+Aβ group. We sought to compare ^{18}F-flortaucipir retention between LBD subjects and AD which necessitated an attempt to control for the effects of both age and disease severity. Given that the LBD cohort was generally younger with relatively preserved MMSE, there were a low number of ADNI subjects who had underwent ^{18}F-flortaucipir PET scans and met our criteria at the time this dataset was downloaded. Although the difference in MMSE between AD and LBD groups was statistically nonsignificant, a larger standard deviation in the AD+Aβ group is noted. By using these strict criteria that selected for younger and less impaired ADNI cases, some of the AD+Aβ cases had low levels of ^{18}F-flortaucipir retention and likely A+/T−/N− or A+/T−/N+ patients (Jack et al., 2016). In spite of this stringent approach, we still saw higher global retention in the AD+Aβ group than LBD−Aβ and HC−Aβ subjects and robust differences in regional ^{18}F-flortaucipir retention in areas known to be affected by AD tau pathology as others have using patient cohorts with greater cognitive impairment (Fleisher et al., 2020; Lee et al., 2018; Nasrallah et al., 2018; Ossenkoppele et al., 2018, 2016; Pontecorvo et al., 2017; Whitwell et al., 2017). Thus, more permissive inclusion will likely only strengthen the findings seen here, but studies with larger cohorts of patients with multi-modal characterization will still be necessary to confirm these findings. ^{18}F-flortaucipir is known to have off-target binding affecting the choroid plexus, and while we attempt to correct for this using PVC values in our primary analysis, some effect on our findings cannot be fully ruled out. We did not observe any significant differences in our analyses when using PVC or non-PVC values from either method described here, suggesting a minimal effect of off-target binding on the observed results (Supplemental Table 2). Although we observe differential retention in hippocampus between AD and LBD, and interpretation of hippocampus retention requires caution due to well-established off-target choroid plexus retention, we have no reason to expect that this off-target retention would be different across groups. Although there are unavoidable time delays between in vivo imaging and postmortem assessments, we had a short PET-autopsy interval in these patients (5 and 8 months) and our regional ROI measures approximate postmortem sampling to enhance imaging-path correlations (Giannini et al., 2019; Irwin et al., 2016a, Irwin et al., 2017b; McMillan et al., 2013, 2016). At this time, neuropathologic results should be viewed as preliminary and larger postmortem validation studies in LBD are needed to confirm our observations (Lowe et al., 2019). Finally, the accumulation of these pathologies in the brain are dynamic processes and longitudinal data in patients followed to autopsy are necessary to clarify the progression of plaque and tangle pathology in LBD. As current efforts in AD focus on biologically driven subgroups (i.e., Amyloid/Tau/Neurodegeneration; A/T/N framework; Jack et al., 2016) to facilitate homogeneity in clinical trials, a similar research approach in LBD may help identify patients with mixed pathology and worse prognosis. This report provides new data suggesting ^{18}F-flortaucipir may have a role in detecting tau copathology in LBD with cognitive impairment and subsequent studies are warranted to address its clinical relevance.

Disclosure statement

Siderowf was a full time employee of AVID radiopharmaceuticals from July 2012 to June 2017.

CRediT authorship contribution statement

David G. Coughlin: Conceptualization, Formal analysis, Data curation, Investigation, Writing - original draft, Writing - review & editing, Visualization. **Jeffrey S. Phillips:** Formal analysis, Investigation, Data curation, Visualization, Writing - review & editing. **Emily Roll:** Data curation, Visualization. **Claire Peterson:** Data curation, Visualization, Software, Methodology. **Rebecca Lobrovich:** Data curation, Investigation, Visualization. **Katya Rascovsky:** Investigation. **Molly Ungrady:** Investigation. **David A. Wolk:** Investigation, Visualization, Funding acquisition. **Sandhitsu Das:** Investigation, Visualization. **Daniel Weintraub:** Investigation. **Edward B. Lee:** Investigation. **John Q. Trojanowski:** Investigation, Writing - review & editing, Funding acquisition. **Sanjeev Vaishnavi:** Investigation. **Andrew Siderowf:** Investigation. **Ilya M. Nasrallah:** Investigation, Visualization, Writing - review & editing. **David J. Irwin:** Conceptualization, Formal analysis, Resources, Writing - review & editing, Visualization, Supervision, Methodology, Project administration. **Corey T. McMillan:** Formal analysis, Data curation, Project administration, Visualization, Writing - review & editing.

Acknowledgments:

Dr. Coughlin is currently affiliated with the University of California San Diego Department of Neurosciences; however, the original work was performed while he was employed at the University of Pennsylvania. Data collection and sharing for this project was funded by the Alzheimer's Disease Neuroimaging Initiative (ADNI) (National Institutes of Health Grant U01 AG024904) and DOD ADNI (Department of Defense award number W81XWH-12-2-0012). ADNI is funded by the National Institute on Aging, the National Institute of Biomedical Imaging and Bioengineering, and through generous contributions from the following: AbbVie, Alzheimer's Association; Alzheimer's Drug Discovery Foundation; Araclon Biotech; BioClinica, Inc.; Biogen; Bristol-Myers Squibb Company; CereSpir, Inc.; Cogstate; Eisai Inc.; Elan Pharmaceuticals, Inc.; Eli Lilly and Company; EuroImmun; F. Hoffmann-La Roche Ltd and its affiliated company Genentech, Inc.; Fujirebio; GE

Healthcare; IXICO Ltd.; Janssen Alzheimer Immunotherapy Research & Development, LLC.; Johnson & Johnson Pharmaceutical Research & Development LLC.; Lumosity; Lundbeck; Merck & Co., Inc.; Meso Scale Diagnostics, LLC.; NeuroRx Research; Neurotrack Technologies; Novartis Pharmaceuticals Corporation; Pfizer Inc.; Piramal Imaging; Servier; Takeda Pharmaceutical Company; and Transition Therapeutics. The Canadian Institutes of Health Research is providing funds to support ADNI clinical sites in Canada. Private sector contributions are facilitated by the Foundation for the National Institutes of Health (www.fnih.org). The grantee organization is the Northern California Institute for Research and Education, and the study is coordinated by the Alzheimer's Therapeutic Research Institute at the University of Southern California. ADNI data are disseminated by the Laboratory for Neuro Imaging at the University of Southern California. ^{18}F-Flortaucipir was donated by AVID Radiopharmaceuticals.

Funding: This work was supported by funding from the American Academy of Neurology/American Brain Foundation (grant number 2059), National Institutes of Health (grant numbers TL1TR001880, AG010124, AG058732, AG061277, NS088341, and NS053488), the Alzheimer's Association (grant number AARF-16-443681), and AVID Radiopharmaceuticals.

Appendix A. Supplementary data

Supplementary data to this article can be found online at https://doi.org/10.1016/j.neurobiolaging.2020.08.003.

References

Abel, T.J., Rhone, A.E., Nourski, K.V., Kawasaki, H., Oya, H., Griffiths, T.D., Howard 3rd, M.A., Tranel, D., 2015. Direct physiologic evidence of a heteromodal convergence region for proper naming in human left anterior temporal lobe. J. Neurosci. 35, 1513–1520.

Avants, B.B., Tustison, N.J., Song, G., Cook, P.A., Klein, A., Gee, J.C., 2011. A reproducible evaluation of ANTs similarity metric performance in brain image registration. Neuroimage 54, 2033–2044.

Baker, S.L., Harrison, T.M., Maaß, A., La Joie, R., Jagust, W., 2019. Effect of off-target binding on 18F-Flortaucipir variability in healthy controls across the lifespan. J. Nucl. Med. 118, 224113.

Baldo, J.V., Shimamura, A.P., 1998. Letter and category fluency in patients with frontal lobe lesions. Neuropsychology 12, 259–267.

Beekly, D.L., Ramos, E.M., Lee, W.W., Deitrich, W.D., Jacka, M.E., Wu, J., Hubbard, J.L., Koepsell, T.D., Morris, J.C., Kukull, W.A., 2007. The National Alzheimer's Coordinating Center (NACC) database: the uniform data set. Alzheimer Dis. Assoc. Disord. 21, 249–258.

Burack, M.A., Hartlein, J., Flores, H.P., Taylor-Reinwald, L., Perlmutter, J.S., Cairns, N.J., 2010. In vivo amyloid imaging in autopsy-confirmed Parkinson disease with dementia. Neurology 74, 77–84.

Chen, H., Pan, X., Lau, J.K.L., Bickerton, W.L., Pradeep, B., Taheri, M., Humphreys, G., Rotshtein, P., 2016. Lesion-symptom mapping of a complex figure copy task: a large-scale PCA study of the BCoS trial. Neuroimage 11, 622–634.

Clark, C.M., Pontecorvo, M.J., Beach, T.G., Bedell, B.J., Coleman, R.E., Doraiswamy, P.M., Fleisher, A.S., Reiman, E.M., Sabbagh, M.N., Sadowsky, C.H., 2012. Cerebral PET with florbetapir compared with neuropathology at autopsy for detection of neuritic amyloid-β plaques: a prospective cohort study. Lancet Neurol. 11, 669–678.

Coughlin, D.G., Hurtig, H.I., Irwin, D.J., 2019b. Pathological influences on clinical heterogeneity in Lewy body diseases. Mov. Disord. 35, 5–19.

Coughlin, D., Xie, S.X., Liang, M., Williams, A., Peterson, C., Weintraub, D., McMillan, C.T., Wolk, D.A., Akhtar, R.S., Hurtig, H.I., Branch Coslett, H., Hamilton, R.H., Siderowf, A.D., Duda, J.E., Rascovsky, K., Lee, E.B., Lee, V.M., Grossman, M., Trojanowski, J.Q., Irwin, D.J., 2019a. Cognitive and pathological influences of tau pathology in Lewy body disorders. Ann. Neurol. 85, 259–271.

Emerton, B.C., Gansler, D.A., Sandberg, E.H., Jerram, M., 2014. Functional anatomic dissociation of description and picture naming in the left temporal lobe. Brain Imaging Behav. 8, 570–578.

Emre, M., Aarsland, D., Brown, R., Burn, D.J., Duyckaerts, C., Mizuno, Y., Broe, G.A., Cummings, J., Dickson, D.W., Gauthier, S., 2007. Clinical diagnostic criteria for dementia associated with Parkinson's disease. Mov. Disord. 22, 1689–1707.

Fleisher, A.S., Pontecorvo, M.J., Devous, M.D., Lu, M., Arora, A.K., Truocchio, S.P., Aldea, P., Flitter, M., Locascio, T., Devine, M., 2020. Positron emission tomography imaging with [18F] flortaucipir and postmortem assessment of Alzheimer disease neuropathologic changes. JAMA Neurol.

Giannini, L.A., Xie, S.X., McMillan, C.T., Liang, M., Williams, A., Jester, C., Rascovsky, K., Wolk, D.A., Ash, S., Lee, E.B., 2019. Divergent patterns of TDP-43 and tau pathologies in primary progressive aphasia. Ann. Neurol. 85, 630–643.

Gomperts, S.N., Locascio, J.J., Makaretz, S.J., Schultz, A., Caso, C., Vasdev, N., Sperling, R., Growdon, J.H., Dickerson, B.C., Johnson, K., 2016. Tau positron emission tomographic imaging in the Lewy body diseases. JAMA Neurol. 73, 1334–1341.

Hamberger, M.J., Miozzo, M., Schevon, C.A., Morrison, C., Carlson, C., Mehta, A.D., Klein, G.E., McKhann 2nd, G.M., Williams, A.C., 2016. Functional differences among stimulation-identified cortical naming sites in the temporal region. Epilepsy Behav. 60, 124–129.

Hamberger, M.J., Seidel, W.T., Goodman, R.R., Perrine, K., McKhann, G.M., 2003. Temporal lobe stimulation reveals anatomic distinction between auditory naming processes. Neurology 60, 1478–1483.

Han, J.Y., Byun, M.S., Seo, E.H., Yi, D., Choe, Y.M., Sohn, B.K., Choi, H.J., Baek, H., Lee, J.H., Kim, H.J., Woo, J.I., Lee, D.Y., 2015. Functional neural correlates of figure copy and recall task performances in cognitively impaired individuals: an 18F-FDG-PET study. Neuroreport 26, 1077–1082.

Hansen, A.K., Damholdt, M.F., Fedorova, T.D., Knudsen, K., Parbo, P., Ismail, R., Østergaard, K., Brooks, D.J., Borghammer, P., 2017. In vivo cortical tau in Parkinson's disease using 18F-AV-1451 positron emission tomography. Mov. Disord. 32, 922–927.

Irwin, D.J., Brettschneider, J., McMillan, C.T., Cooper, F., Olm, C., Arnold, S.E., Van Deerlin, V.M., Seeley, W.W., Miller, B.L., Lee, E.B., Lee, V.M., Grossman, M., Trojanowski, J.Q., 2016a. Deep clinical and neuropathological phenotyping of Pick disease. Ann. Neurol. 79, 272–287.

Irwin, D.J., Byrne, M.D., McMillan, C.T., Cooper, F., Arnold, S.E., Lee, E.B., Van Deerlin, V.M., Xie, S.X., Lee, V.M., Grossman, M., Trojanowski, J.Q., 2016b. Semi-Automated digital image analysis of pick's disease and TDP-43 proteinopathy. J. Histochem. Cytochem. 64, 54–66.

Irwin, D.J., Grossman, M., Weintraub, D., Hurtig, H.I., Duda, J.E., Xie, S.X., Lee, E.B., Van Deerlin, V.M., Lopez, O.L., Kofler, J.K., Nelson, P.T., Jicha, G.A., Woltjer, R., Quinn, J.F., Kaye, J., Leverenz, J.B., Tsuang, D., Longfellow, K., Yearout, D., Kukull, W., Keene, C.D., Montine, T.J., Zabetian, C.P., Trojanowski, J.Q., 2017a. Neuropathological and genetic correlates of survival and dementia onset in synucleinopathies: a retrospective analysis. Lancet Neurol. 16, 55–65.

Irwin, D.J., McMillan, C.T., Xie, S.X., Rascovsky, K., Van Deerlin, V.M., Coslett, H.B., Hamilton, R., Aguirre, G.K., Lee, E.B., Lee, V.M., 2017b. Asymmetry of post-mortem neuropathology in behavioural-variant frontotemporal dementia. Brain 141, 288–301.

Irwin, D.J., White, M.T., Toledo, J.B., Xie, S.X., Robinson, J.L., Van Deerlin, V., Lee, V.M., Leverenz, J.B., Montine, T.J., Duda, J.E., Hurtig, H.I., Trojanowski, J.Q., 2012. Neuropathologic substrates of Parkinson disease dementia. Ann. Neurol. 72, 587–598.

Irwin, D.J., Xie, S.X., Coughlin, D., Nevler, N., Akhtar, R.S., McMillan, C.T., Lee, E.B., Wolk, D.A., Weintraub, D., Chen-Plotkin, A., Duda, J.E., Spindler, M., Siderowf, A., Hurtig, H.I., Shaw, L.M., Grossman, M., Trojanowski, J.Q., 2018. CSF tau and amyloid-beta predict cerebral synucleinopathy in autopsied Lewy body disorders. Neurology.

Iseki, E., Togo, T., Suzuki, K., Katsuse, O., Marui, W., de Silva, R., Lees, A., Yamamoto, T., Kosaka, K., 2003. Dementia with Lewy bodies from the perspective of tauopathy. Acta Neuropathol. 105, 265–270.

Jack, C.R., Bennett, D.A., Blennow, K., Carrillo, M.C., Feldman, H.H., Frisoni, G.B., Hampel, H., Jagust, W.J., Johnson, K.A., Knopman, D.S., 2016. A/T/N: an unbiased descriptive classification scheme for Alzheimer disease biomarkers. Neurology 87, 539–547.

Jagust, W.J., Landau, S.M., Koeppe, R.A., Reiman, E.M., Chen, K., Mathis, C.A., Price, J.C., Foster, N.L., Wang, A.Y., 2015. The Alzheimer's disease neuroimaging initiative 2 PET core: 2015. Alzheimers Dement. 11, 757–771.

Jellinger, K., Seppi, K., Wenning, G., Poewe, W., 2002. Impact of coexistent Alzheimer pathology on the natural history of Parkinson's disease. J. Neural Transm. 109, 329–339.

Kantarci, K., Lowe, V.J., Boeve, B.F., Senjem, M.L., Tosakulwong, N., Lesnick, T.G., Spychalla, A.J., Gunter, J.L., Fields, J.A., Graff-Radford, J., 2017. AV-1451 tau and β-amyloid positron emission tomography imaging in dementia with Lewy bodies. Ann. Neurol. 81, 58–67.

Klein, A., Ghosh, S.S., Bao, F.S., Giard, J., Häme, Y., Stavsky, E., Lee, N., Rossa, B., Reuter, M., Neto, E.C., 2017. Mindboggling morphometry of human brains. PLoS Comput. Biol. 13, e1005350.

Klein, A., Tourville, J., 2012. 101 labeled brain images and a consistent human cortical labeling protocol. Front. Neurosci. 6, 171.

Kraybill, M.L., Larson, E.B., Tsuang, D., Teri, L., McCormick, W., Bowen, J., Kukull, W., Leverenz, J., Cherrier, M., 2005. Cognitive differences in dementia patients with autopsy-verified AD, Lewy body pathology, or both. Neurology 64, 2069–2073.

La Joie, R., Bejanin, A., Fagan, A.M., Ayakta, N., Baker, S.L., Bourakova, V., Boxer, A.L., Cha, J., Karydas, A., Jerome, G., Maass, A., Mensing, A., Miller, Z.A., O'Neil, J.P., Pham, J., Rosen, H.J., Tsai, R., Visani, A.V., Miller, B.L., Jagust, W.J., Rabinovici, G.D., 2018. Associations between [(18)F]AV1451 tau PET and CSF measures of tau pathology in a clinical sample. Neurology 90, e282–e290.

Landau, S.M., Breault, C., Joshi, A.D., Pontecorvo, M., Mathis, C.A., Jagust, W.J., Mintun, M.A., 2013. Amyloid-β imaging with Pittsburgh compound B and florbetapir: comparing radiotracers and quantification methods. J. Nucl. Med. 54, 70–77.

Lee, S.H., Cho, H., Choi, J.Y., Lee, J.H., Ryu, Y.H., Lee, M.S., Lyoo, C.H., 2018. Distinct patterns of amyloid-dependent tau accumulation in Lewy body diseases. Mov. Disord. 33, 262–272.
Litvan, I., Aarsland, D., Adler, C.H., Goldman, J.G., Kulisevsky, J., Mollenhauer, B., Rodriguez-Oroz, M.C., Tröster, A.I., Weintraub, D., 2011. MDS task force on mild cognitive impairment in Parkinson's disease: critical review of PD-MCI. Mov. Disord. 26, 1814–1824.
Lowe, V.J., Lundt, E.S., Albertson, S.M., Min, H.-K., Fang, P., Przybelski, S.A., Senjem, M.L., Schwarz, C.G., Kantarci, K., Boeve, B., 2019. Tau-positron emission tomography correlates with neuropathology findings. Alzheimers Dement.
Marquié, M., Normandin, M.D., Vanderburg, C.R., Costantino, I.M., Bien, E.A., Rycyna, L.G., Klunk, W.E., Mathis, C.A., Ikonomovic, M.D., Debnath, M.L., 2015. Validating novel tau positron emission tomography tracer [F-18]-AV-1451 (T807) on postmortem brain tissue. Ann. Neurol. 78, 787–800.
Mattsson, N., Smith, R., Strandberg, O., Palmqvist, S., Scholl, M., Insel, P.S., Hagerstrom, D., Ohlsson, T., Zetterberg, H., Blennow, K., Jogi, J., Hansson, O., 2018. Comparing (18)F-AV-1451 with CSF t-tau and p-tau for diagnosis of Alzheimer disease. Neurology 90, e388–e395.
McConley, R., Martin, R., Palmer, C.A., Kuzniecky, R., Knowlton, R., Faught, E., 2008. Rey Osterrieth complex figure test spatial and figural scoring: relations to seizure focus and hippocampal pathology in patients with temporal lobe epilepsy. Epilepsy Behav. 13, 174–177.
McKeith, I.G., Boeve, B.F., Dickson, D.W., Halliday, G., Taylor, J.-P., Weintraub, D., Aarsland, D., Galvin, J., Attems, J., Ballard, C.G., 2017. Diagnosis and management of dementia with Lewy bodies: fourth consensus report of the DLB Consortium. Neurology 89, 88–100.
McKeith, I.G., Dickson, D.W., Lowe, J., Emre, M., O'Brien, J.T., Feldman, H., Cummings, J., Duda, J.E., Lippa, C., Perry, E.K., Aarsland, D., Arai, H., Ballard, C.G., Boeve, B., Burn, D.J., Costa, D., Del Ser, T., Dubois, B., Galasko, D., Gauthier, S., Goetz, C.G., Gomez-Tortosa, E., Halliday, G., Hansen, L.A., Hardy, J., Iwatsubo, T., Kalaria, R.N., Kaufer, D., Kenny, R.A., Korczyn, A., Kosaka, K., Lee, V.M., Lees, A., Litvan, I., Londos, E., Lopez, O.L., Minoshima, S., Mizuno, Y., Molina, J.A., Mukaetova-Ladinska, E.B., Pasquier, F., Perry, R.H., Schulz, J.B., Trojanowski, J.Q., Yamada, M., 2005. Diagnosis and management of dementia with Lewy bodies: third report of the DLB Consortium. Neurology 65, 1863–1872.
McMillan, C.T., Chételat, G., 2018. Amyloid "accumulators": the next generation of candidates for amyloid-targeted clinical trials? Neurology 90, 759–760.
McMillan, C.T., Irwin, D.J., Avants, B.B., Powers, J., Cook, P.A., Toledo, J.B., Wood, E.M., Van Deerlin, V.M., Lee, V.M., Trojanowski, J.Q., 2013. White matter imaging helps dissociate tau from TDP-43 in frontotemporal lobar degeneration. J. Neurol. Neurosurg. Psychiatry 84, 949–955.
McMillan, C.T., Irwin, D.J., Nasrallah, I., Phillips, J.S., Spindler, M., Rascovsky, K., Ternes, K., Jester, C., Wolk, D.A., Kwong, L.K., Lee, V.M., Lee, E.B., Trojanowski, J.Q., Grossman, M., 2016. Multimodal evaluation demonstrates in vivo (18)F-AV-1451 uptake in autopsy-confirmed corticobasal degeneration. Acta Neuropathol. 132, 935–937.
McMillan, C.T., Wolk, D.A., 2016. Presence of cerebral amyloid modulates phenotype and pattern of neurodegeneration in early Parkinson's disease. J. Neurol. Neurosurg. Psychiatry 87, 1112–1122.
Montine, T.J., Phelps, C.H., Beach, T.G., Bigio, E.H., Cairns, N.J., Dickson, D.W., Duyckaerts, C., Frosch, M.P., Masliah, E., Mirra, S.S., Nelson, P.T., Schneider, J.A., Thal, D.R., Trojanowski, J.Q., Vinters, H.V., Hyman, B.T., National Institute on, A., Alzheimer's, A., 2012. National Institute on Aging-Alzheimer's Association guidelines for the neuropathologic assessment of Alzheimer's disease: a practical approach. Acta Neuropathol. 123, 1–11.
Moscovitch, M., 1994. Cognitive Resources and dual-task interference effects at retrieval in normal people: the role of the frontal lobes and medial temporal cortex. Neuropsychology 8, 524.
Nasrallah, I.M., Chen, Y.J., Hsieh, M.-K., Phillips, J.S., Ternes, K., Stockbower, G.E., Sheline, Y., McMillan, C.T., Grossman, M., Wolk, D.A., 2018. 18F-Flortaucipir PET/MRI correlations in nonamnestic and amnestic variants of Alzheimer disease. J. Nucl. Med. 59, 299–306.
Ossenkoppele, R., Rabinovici, G.D., Smith, R., Cho, H., Schöll, M., Strandberg, O., Palmqvist, S., Mattsson, N., Janelidze, S., Santillo, A., 2018. Discriminative accuracy of [18F] flortaucipir positron emission tomography for Alzheimer disease vs other neurodegenerative disorders. JAMA 320, 1151–1162.
Ossenkoppele, R., Schonhaut, D.R., Schöll, M., Lockhart, S.N., Ayakta, N., Baker, S.L., O'Neil, J.P., Janabi, M., Lazaris, A., Cantwell, A., 2016. Tau PET patterns mirror clinical and neuroanatomical variability in Alzheimer's disease. Brain 139, 1551–1567.
Peavy, G.M., Edland, S.D., Toole, B.M., Hansen, L.A., Galasko, D.R., Mayo, A.M., 2016. Phenotypic differences based on staging of Alzheimer's neuropathology in autopsy-confirmed dementia with Lewy bodies. Parkinsonism Relat. Disord. 31, 72–78.
Pontecorvo, M.J., Devous Sr, M.D., Navitsky, M., Lu, M., Salloway, S., Schaerf, F.W., Jennings, D., Arora, A.K., McGeehan, A., Lim, N.C., 2017. Relationships between flortaucipir PET tau binding and amyloid burden, clinical diagnosis, age and cognition. Brain 140, 748–763.
Quinn, C., Elman, L., McCluskey, L., Hoskins, K., Karam, C., Woo, J.H., Poptani, H., Wang, S., Chawla, S., Kasner, S.E., Grossman, M., 2012. Frontal lobe abnormalities on MRS correlate with poor letter fluency in ALS. Neurology 79, 583–588.
Rizzo, G., Arcuti, S., Copetti, M., Alessandria, M., Savica, R., Fontana, A., Liguori, R., Logroscino, G., 2018. Accuracy of clinical diagnosis of dementia with Lewy bodies: a systematic review and meta-analysis. J. Neurol. Neurosurg. Psychiatry 89, 358–366.
Rizzo, G., Copetti, M., Arcuti, S., Martino, D., Fontana, A., Logroscino, G., 2016. Accuracy of clinical diagnosis of Parkinson disease: a systematic review and meta-analysis. Neurology 86, 566–576.
Roalf, D.R., Moberg, P.J., Xie, S.X., Wolk, D.A., Moelter, S.T., Arnold, S.E., 2013. Comparative accuracies of two common screening instruments for classification of Alzheimer's disease, mild cognitive impairment, and healthy aging. Alzheimers Dement. 9, 529–537.
Rousset, O.G., Ma, Y., Evans, A.C., 1998. Correction for partial volume effects in PET: principle and validation. J. Nucl. Med. 39, 904–911.
Shaw, L.M., Vanderstichele, H., Knapik-Czajka, M., Clark, C.M., Aisen, P.S., Petersen, R.C., Blennow, K., Soares, H., Simon, A., Lewczuk, P., 2009. Cerebrospinal fluid biomarker signature in Alzheimer's disease neuroimaging initiative subjects. Ann. Neurol. 65, 403–413.
Smith, R., Scholl, M., Londos, E., Ohlsson, T., Hansson, O., 2018. (18)F-AV-1451 in Parkinson's disease with and without dementia and in dementia with Lewy bodies. Sci. Rep. 8, 4717.
Thomas, B.A., Cuplov, V., Bousse, A., Mendes, A., Thielemans, K., Hutton, B.F., Erlandsson, K., 2016. PETPVC: a toolbox for performing partial volume correction techniques in positron emission tomography. Phys. Med. Biol. 61, 7975.
Toledo, J.B., Van Deerlin, V.M., Lee, E.B., Suh, E., Baek, Y., Robinson, J.L., Xie, S.X., McBride, J., Wood, E.M., Schuck, T., Irwin, D.J., Gross, R.G., Hurtig, H., McCluskey, L., Elman, L., Karlawish, J., Schellenberg, G., Chen-Plotkin, A., Wolk, D., Grossman, M., Arnold, S.E., Shaw, L.M., Lee, V.M., Trojanowski, J.Q., 2014. A platform for discovery: the university of Pennsylvania integrated Neurodegenerative Disease Biobank. Alzheimers Dement. 10, 477–484.
Tsai, R.M., Bejanin, A., Lesman-Segev, O., LaJoie, R., Visani, A., Bourakova, V., O'Neil, J.P., Janabi, M., Baker, S., Lee, S.E., 2019. 18 F-flortaucipir (AV-1451) tau PET in frontotemporal dementia syndromes. Alzheimers Res. Ther. 11, 13.
Vemuri, P., Lowe, V.J., Knopman, D.S., Senjem, M.L., Kemp, B.J., Schwarz, C.G., Przybelski, S.A., Machulda, M.M., Petersen, R.C., Jack Jr., C.R., 2017. Tau-PET uptake: regional variation in average SUVR and impact of amyloid deposition. Alzheimers Dement. 6, 21–30.
Wakisaka, Y., Furuta, A., Tanizaki, Y., Kiyohara, Y., Iida, M., Iwaki, T., 2003. Age-associated prevalence and risk factors of Lewy body pathology in a general population: the Hisayama study. Acta Neuropathol. 106, 374–382.
Wang, H., Suh, J.W., Das, S.R., Pluta, J.B., Craige, C., Yushkevich, P.A., 2013. Multi-atlas segmentation with joint label fusion. IEEE Trans. Pattern Anal. Mach. Intell. 35, 611–623.
Watson, G.S., Cholerton, B.A., Gross, R.G., Weintraub, D., Zabetian, C.P., Trojanowski, J.Q., Montine, T.J., Siderowf, A., Leverenz, J.B., 2013. Neuropsychologic assessment in collaborative Parkinson's disease research: a proposal from the National Institute of Neurological Disorders and Stroke Morris K. Alzheimers Dement. 9, 609–614.
Weiner, M.W., Veitch, D.P., Aisen, P.S., Beckett, L.A., Cairns, N.J., Green, R.C., Harvey, D., Jack Jr., C.R., Jagust, W., Morris, J.C., 2017. The Alzheimer's Disease Neuroimaging Initiative 3: continued innovation for clinical trial improvement. Alzheimers Dement. 13, 561–571.
Whitwell, J.L., Lowe, V.J., Tosakulwong, N., Weigand, S.D., Senjem, M.L., Schwarz, C.G., Spychalla, A.J., Petersen, R.C., Jack Jr., C.R., Josephs, K.A., 2017. [18 F]AV-1451 tau positron emission tomography in progressive supranuclear palsy. Mov. Disord. 32, 124–133.
Whitwell, J.L., Tosakulwong, N., Botha, H., Ali, F., Clark, H.M., Duffy, J.R., Utianski, R.L., Stevens, C.A., Weigand, S.D., Schwarz, C.G., 2020. Brain volume and flortaucipir analysis of progressive supranuclear palsy clinical variants. Neuroimage 25, 102152.
Winer, J.R., Maass, A., Pressman, P., Stiver, J., Schonhaut, D.R., Baker, S.L., Kramer, J., Rabinovici, G.D., Jagust, W.J., 2018. Associations between tau, β-amyloid, and cognition in Parkinson disease. JAMA Neurol. 75, 227–235.
Xu, J., Guan, X., Li, H., Xu, X., Zhang, M., 2019. Integration and segregation of functional segmented anterior and posterior hippocampal networks in memory performance. Behav. Brain Res. 364, 256–263.
Zammit, A.R., Ezzati, A., Katz, M.J., Zimmerman, M.E., Lipton, M.L., Sliwinski, M.J., Lipton, R.B., 2017a. The association of visual memory with hippocampal volume. PLoS One 12, e0187851.
Zammit, A.R., Ezzati, A., Zimmerman, M.E., Lipton, R.B., Lipton, M.L., Katz, M.J., 2017b. Roles of hippocampal subfields in verbal and visual episodic memory. Behav. Brain Res. 317, 157–162.